Load and Deformation Relations of Placed Riprap Model with Toe Support

Théo Dezert[1], Ganesh Ravindra[1,2] and Fjóla Sigtryggsdottir[1]

[1] Norwegian University of Science and Technology – Department of Civil and Environmental Engineering, Trondheim, Norway,
theo.dezert@ntnu.no, fjola.g.sigtryggsdottir@ntnu.no

[2] Trondheim Kommune– Department of Water and Wastewater, Trondheim, Norway,
ganesh.hiriyanna.rao.ravindra@trondheim.kommune.no

Abstract

Rockfill dams are hydraulic structures of major importance that can be exposed to extreme flood events,leading to overtopping processes. These phenomena erode and weaken their structural and geotechnical stability. As a rockfill dam protection, ripraps are broadly used against erosion processes. For steep slopes, as the one considered in this work, riprap failure is made possible during overtopping process. Thus, understanding the riprap behavior during overtopping events is a major issue to improve construction and reinforcement techniques.In this work, datasets were obtained from an experimental model of placed riprap built in a flume. The riprap stoneswereplaced in an interlocking pattern with a metallic support at the toe. The modelwas submitted to successive overtoppingwith increasing levels of discharge until its complete failure. A laser traverse system measured the coordinates of specific riprap stones between each discharge increase and six load cells located at the toe measured the load during the entire procedure. From the total load values, two different types of load contributions could be distinguished: the self-weight of the stones and the hydraulic load depending on the discharge level of the overflow. The present work highlightsthe strong relation between riprap stone displacements and axial reaction load values measured at the toe. The results demonstrate that as the hydraulic load induces 2D deformations of the riprap, a larger part of the riprap weight is supported at the toe. Thus, the measured axial load during overtopping arises both from the hydraulic load and from the load imputed to the compaction of the riprap layer.This compaction effect induces an even greater load than the oneimputed to the water.

Keywords: Riprap Stability; Hydraulic Model; Overtopping; Toe Support; Displacement

1. INTRODUCTION

Ripraps are protection structures against erosion and scouring, widely used to protect various civil engineering structures such as dams, levees, spillways, bridge piers, channel beds (Abt et al., 2013; Hiller et al., 2018a; Johnson et al., 2013; Najafzadeh et al., 2018; Siebel, 2007). These structures are composed of many large rocks and an important issue in Norway is the understanding of riprap stability in the context of rockfill dams. In particular, ripraps are used to resist against external erosion associated with overtopping phenomena. Thus, it is important to understand the rupture mechanisms of the riprap protecting these structures since overtopping events are responsible for most structural failure cases.

Two main types of riprap construction can be encountered: dumped riprap and placed riprap. While dumped riprap are made of randomly placed stones lying on the dam shoulder, placed riprap are defined by a specific arrangement of stones. In the field of riprap study, previous experimental models have already been set up in the hydraulic laboratory of the Norwegian University of Science and Technology. Hiller et al. (2018a) investigated the failure process of placed riprap stones on a ramp supported at the toe section and exposed to successive overtopping, anddemonstrated that placed riprap with such support is more resistant against overtopping than dumped riprap. Conversely, Ravindra et al. (2021) demonstrated the existence of a buckling phenomenon of suchtoe-supported riprap layer by examining the 2D displacement of riprap stones as a function of the level of overtopping water discharge.Furthermore, Ravindra et al. (2020) investigated the failure mechanism of placed riprap without toe support.

This paperpresents results from amodel as the ones built in Hiller et al. (2018a) and Ravindra et al. (2021), adding load cells on the toe support to measure axial reaction load values during experimental testing. Here, the aim is to understand the relation between axial load measured at the toe, riprap stone displacement and water discharge level on a placed riprap model with toe support. Such toe supports could be of interest to reinforce actual dams against overtopping phenomena. First, the experimental model structure is introduced

as well as the overtopping procedure and the types of recorded data. Then, the load values recorded during riprap construction are presented and discussed, as well as their values during overtopping testing and their relation with discharge values and riprap stone displacements.

2. EXPERIMENTAL MODEL, PROCEDURE AND DATA

2.1 Riprap model

The experimental modeldisplayed in this work is as the ones introduced in Hiller et al. (2018a) and in Ravindra et al. (2021). Thus, more information can be found in these two-prior works.The considered modelwasbuilt at the hydraulic laboratory (Norwegian University of Science and Technology, Trondheim) in a 25 m long, 2 m high and 1 m wide horizontal flume.

The experimental model is a 1:10 scale model of a riprap layer built on the downstream side of a dam (Figure 1.a),the construction was designed by Hiller et al. (2018a) assuming Froude similarity. The riprap layer lies on a filter layer built on an inclined rampwith a slope of 1:1.5 (S=0.67), Figure 1.b. The filter and the riprapwerearranged across the whole width of the flume (1 m), for a total chute length of L_s=1.75 m. The length of the horizontal crest is 0.55 m. A metallic element was fixed at the toe to support the structure. Also, the whole experimental model was elevated from the base of the flume to prevent from backwater effects and to focus only on rupture and erosion of riprap from overtopping processes.

A test was carried out with placed riprap stonesarranged on a filter layer(thickness of 0.1 m)made of a layer of angular stones and a geotextile. Over the filter, the single riprap layer was built by positioningaround1 100 stones from the toe section up to the crest, respecting an interlocking pattern. According to Bunte and Abt (2001), the nominal diameter can be defined as $d = (abc)^{1/3}$with a the longest, b the intermediate and $c$the shortest axis of a stone. Considering this, the filter layer consisted of stones with nominal diameter of $d_{50, F}$ = 0.025 m and density of $Á_{s,F}$= 3050 kg.m^{-3}. The riprap layer consisted of larger rhyolite stones with nominal diameter of d_{50} = 0.053 m (a=0.088 m, b=0.049 m and c=0.036 m) and density of $Á_s$=2710kg.m^{-3}.These riprap stones were arrangedaccording to an angle of ² H 60° (Figure 1.b) between the a-axis and the chute bottom while the crest stones were arrangedaccording to an angle of² H 90° (Lia et al., 2013). The dimensioning of filter and riprap layers were suggested according to the Norwegian Water Resources and Energy Directorate guidelines (NVE, 2012).
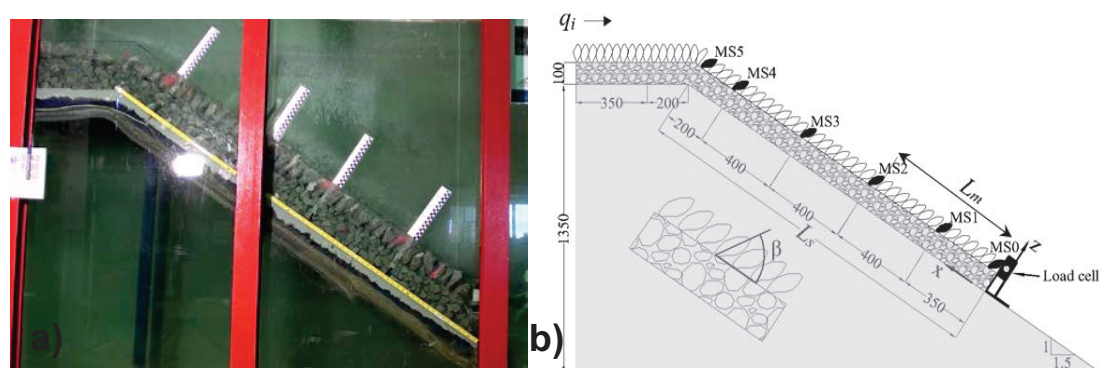

Figure 1. a) Picture of the experimental model before overtopping, b) representation of the test set-up with corresponding lengths and positions of marked riprap stones (MS0-5), adapted from Ravindra et al. (2020).

2.2 Overtopping methodology

Successive overtopping were carried out on the model thanks to pumps of a combined capacity of q_p = 400 l.s^{-1}.The first overtopping started at an initial discharge roughly equal toq_i = 50 l.s^{-1}. Then, the discharge $q_i$was successively increased for a fixed time interval of 1800 s, within a range of 20 - 50 l.s^{-1}.The exact recorded discharge values are displayed in Table 1. The procedure was repeated until the rupture of the model. The water flow was interrupted between each discharge increase, and we defined q_c as the critical discharge value for which a complete failure of the riprap layeris observed (for the 11th discharge step, Table 1).

Table 1. Number of discharge step and corresponding recorded values until failure of the model.

Number of discharge step	1	2	3	4	5	6	7	8	9	10	11
Discharge (l.s^{-1})	52	100	126	150	175	200	224	251	275	300	325

2.3 Types of data

Six riprap stones, located along the central axis of the riprap slope, were chosen and marked (Figure 1.b). They were identified as MS0, MS1, MS2, MS3, MS4 and MS5 and placed so that x = 0, 0.35, 0.75, 1.15, 1.55 and 1.75 m respectively. Theircoordinates were recorded with an automated 3D-traverse laserlocated above the model. The positioning was done in a 3D Cartesian coordinate system with the origin being located at the toe. The x-axis is parallel to the chute, pointing in the upstream direction whilethe z-axis is perpendicular to the ramp (Figure 1.b). The accuracy of the measurements are around 0.1 mm and 1 mm in x and z directions respectively. The riprap stone displacements were only recorded along x and z-axis before each discharge increment when the water flow was interrupted.

Load values, F_i, were also recorded with 6 load cells (S9M force transducer manufactured by HBM) positioned at the toe of the experimental model (Figure 1.b).The combined capacity of these cells is 3 kN.Contrary to the laser recording, the recording of the loaddata was possible throughout the test between each overtopping step, but also while the water was flowing and during the building of the riprap structure. Here,F_c, is defined as the critical load valuefor which a complete failure of the model occurs.

3. RESULTS

3.1 Axial reaction load during riprap construction

The axial reactionload at the supported toe were recorded while the riprap layer was being built. The reaction loads measured represent the part of the component of the riprap weight parallel to the slope that is not resisted by frictional forces.These measured values are displayed, according to the length from the toe, in Figure 2. These data display the fast load increase during the building of about the first 50 cm of the riprap layer (almost 1/3rd of the chute length). The load then stabilizes to an average value of 110 N. These results suggest that the component of the riprap weight parallel to the slope for the first layers, placed directly against the support, is largely carried by the toe support or untila threshold length is reached when the frictional resistance governs.
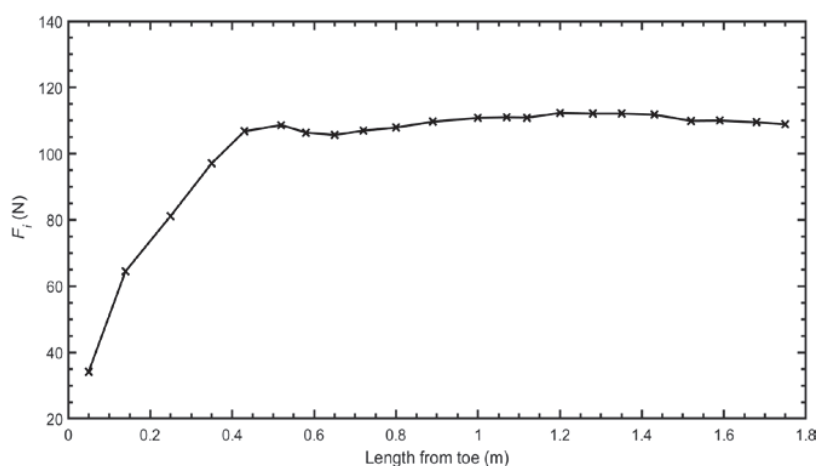

Figure 2. Axial load at the toe section of the experimental model during riprap layer construction.

3.2 Axial reaction load during testing

After the buildingphase, the pumps were turned on and the water flow could overtop the riprap model and generate an increase of the loadat the toe. Axial reaction load values$F_i$were recorded and are displayed in Figure 3 according to water discharge values.

Since between each discharge step the water flow was stopped, it is also possible to plot the load values of the compaction effect. These are basically the measured values when no water is flowing over the model after each discharge step. Indeed, even though the total load increases along with the discharge level (in

black, Figure 3), the loads imputed to the riprap compaction effect (in red, Figure 3) also increase after each discharge step, without any water flowing. It can be observed that these values do not come back to their previous values before overtopping. These results suggest that not only the increase of the water discharge induces a load increase but also that the riprap stone displacement and their compaction generate an increase of the load. Thus, the total load (in black, Figure 3) measured at the toe is composed of the load from stone compaction effect (in red, Figure 3) and the hydraulic load imputed to the water effect (in blue, Figure 3).
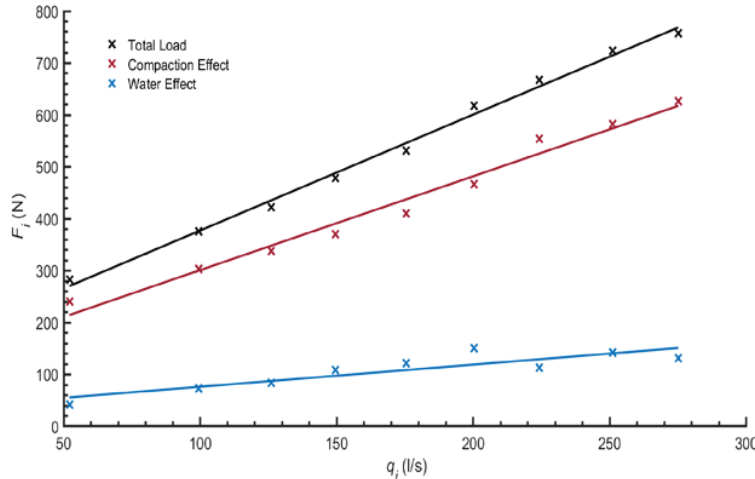

Figure 3. Load at the toe section of the experimental model during testing.

A strong linear relation exists between total loads at the toe section and the water discharge values (Nash-Sutcliffe coefficients R^2 close to 1). From this experimental test, theexpressiondescribing the relation between the discharge level and the load at the toe section can be written as:

$$F_i = 2.235\, q_i + 153.9 \ [1]$$

3.3 1D riprap stone displacement

The movements of the marked riprap stones according to load valuesalong the x-axis are displayed in Figure 4. This had been previously done in Hiller et al. (2018a) and Ravindra et al. (2021) according to water discharge values.
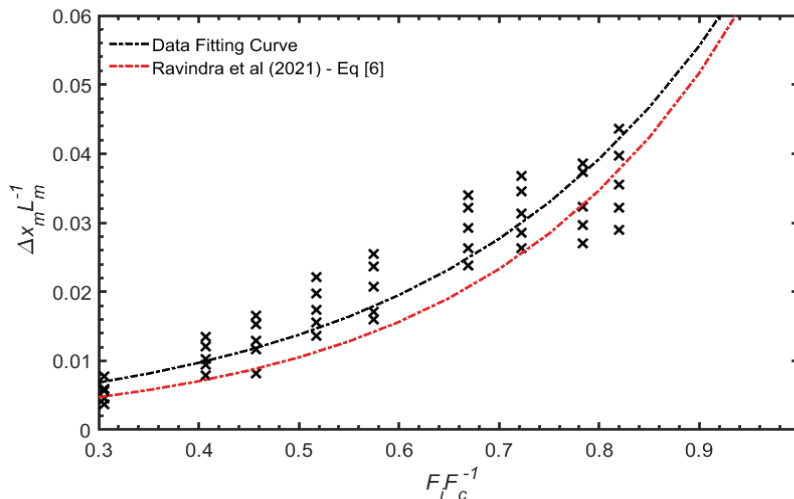

Figure 4. Riprap marked stone displacement along x-axis according to normalized load values at the toe section.

Here, the stone displacement is normalized by $\Delta x_m / L_m$(Larsen et al., 1986) with$L_m = x_m - x_0$, where$m$denotes the position of one of the fivemarked riprap stone along x-axis (1-5). The displacement Δx_m corresponds to the difference between the actual positionof a stone andits initial position, before the first overtopping. In Figure 4,

the 1D stone displacement is analyzed according to the critical unit load ($F_iF_c^{-1}$) with F_c = 924 N. The stone displacements areexamined according to the position of the riprap stone located at the bottom of the riprap layer and identified as MS0, as it was done in Ravindra et al. (2021). Becausethis specific stone is maintained by the fixed toe support, it undergoes very moderate movement.

The displayed results suggest an exponential relationship (with R^2 H 0.85) between these two parameters (dotted curve in Figure 4). The stone displacements along x-axis increase with the measured load. As a comparison, the relation between ” $x_m/L_m$and $q_iq_c^{-1}$ proposed by Ravindra et al. (2021) (cfEq[6] of the article), was plotted in red (Figure 4).

3.4 2D riprap stone displacement

The 2D movements of marked riprap stones were also computed according to load values measured at the toe section. The results are displayed in Figure 5, with the horizontal axis standing for $L_m$normalized over the total riprap length $L_s$and the vertical axis ” $z_md_{50}^{-1}$standing for the stone displacement along the z-axis over the nominal riprap stone diameter. These results display a progressive displacement in both$z$ and x directions along with the increase of the load. The stones of the riprap layer tend to go downstream along the x-axis (compaction of the riprap) but also to elevate in the z-direction. These movementsappear to be directly related to the magnitude of the measured load. Furthermore, the magnitude of the elevation (z-direction)appears to depend on the riprap stone position on the ramp and relate to buckling of columns (Ravindra et al, 2021). The compaction of the riprap layer, imputed to the overtopping,induces the generation of a gap at the upstream part of the riprap layer. Since the support at the toe hinders sliding of the slope, the buckling like deformation in the z-direction leads to the complete failure of the model after successive overtopping events.
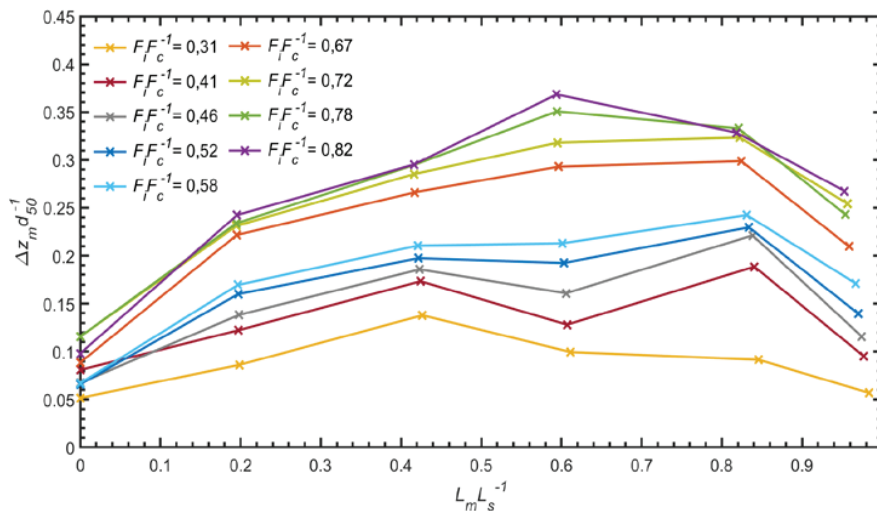

Figure 5. Riprap marked stone displacement along x-axis and z-axis according to normalized load values at the toe section.

4.   DISCUSSION

From the results displayed in this study, it is firstinteresting to point out that a stabilization of the reaction load measured at the toe is observed soon during the riprap layer construction (Figure 2). Indeed, the interlocking pattern of the riprap stones and the friction with the filter layer could explain such behavior. As mentioned in Hiller et al. (2018b), the interlocking of the riprap stones enables the transfer of longitudinal forces within the whole layer. From results obtained on experimental model without toe support (Ravindra et al., 2020), the specificity of this type of riprap also explains why it can resist to 1.5 times greater discharge values (water loads) than dumped riprap structure.

The results from Figure 3 also bring out an important information. They point out that even though the discharge level plays an important role in the load measured at the toe, the increase of load which is imputed to the riprap deformation layer is greater than the contribution from the water flow. This means that both the compression (displayed in Figure 4) and the elevation (displayed in Figure 5) of the riprap stones induce an additional load. The compression along the x-axis can be imputed to both the gravity and hydraulic drag and lift forces during the overtopping stages. The hydraulic lift force also tends to elevate the stones in the z-direction, while the interlocking forces tend to vertically counter that effect.However, the measured elevation in the z-direction after each overtopping stage is attributed to the buckling like behavior of the riprap structure,

with these interlocking forces generating a bearing structure that can resist important loads, particularly when supported at the toe.

The results obtained from this study globally demonstrate a strong relation between axial reaction load at the toe section and deformation of the riprap layer on an experimental model. Ravindra et al. (2021) pointed out a buckling analogy for 2D deformation of placed riprap supported at the toe when exposed to overtopping. Here, the buckling process can also be observed from results displayed in Figure 5 when compared to load values. This makes this study consistent with previous research works and helps to understand the results from Figure 3. As a matter of fact, the relative elevation of riprap stones from the middle of the structure in comparison to the stones from the toe (Figure 5) could be describe as an increase of the slope of the riprap column. Taking into consideration that the elevation of the stones induces less friction on the filter layer, these two processesresult in that a larger part of the riprap weight (component parallel to the slope) is carried by the support.Also, the compaction of the riprap against the toe support induces an increase of the reaction load in the x-direction (axial load), perpendicular to the metallic toe support where the load cells are located.Thus, both the compaction and elevation of the riprap stones are responsible for the load increase at the toe.

Even though these first results are encouraging, they should be considered carefully since the data were collected from only one experimental test. More data issued from other tests aim to be analyzed and published to attest the validity of this research work. Furthermore, in future studies, it would be valuable to modify some of the experimental parameters such as the slope value and the nature of the stones to understand the limitations of the studied structural behavior. Building a rockfill dam shoulder below the filter layer instead of a ramp would also be of great interest to understand the impact of the throughflow on the relation between riprap stone displacement and load values. Such study could be a valuable contribution to the recent work from Kiplesund et al. (2021) focused on throughflow properties of rockfill dams.

5. CONCLUSIONS

In this work, we displayed and discussed the results obtained from overtopping testing on an experimental model built in the hydraulic laboratory of the Norwegian University of Science and Technology. The model consisted of placed riprap stones supported at the toe and lying on a filter layer built on a ramp with a steep slope (S = 0.67). The testing procedure consisted of successive overtopping water discharge with increasing level until complete failure of the structure.

This study demonstrated that strong relations between load at the toe, riprap stone displacement and discharge level exist. The deformation of the riprap layer that was qualified as "buckling deformation" in Ravindra et al. (2021) was observed. It progressively induced an increase of the load measured at the toe. It also appeared that the contribution of the load induced by the riprap displacement is greater than the contribution of the hydraulic load from the water flow. Furthermore, a very strong relation between discharge values and load at the toe has been demonstrated such as a relation between riprap stone compression and load values. It was high lightened that the interlocking pattern of the placed riprap stones acts as a bearing structure and induced a stabilization of the load value at the toe during the construction stage.

Such results, when corroborated by additional test data, could be valuable to improve the understanding of riprap stability on rockfill dams as well as to provide suggestions for dam reinforcement techniques.

6. ACKNOWLEDGEMENT

7. REFERENCES

Abt, S.R., Thornton, C.I., Scholl, B.A. and Bender, T.R. (2013). Evaluation ofovertopping riprap design relationships. *Journal of the American Water ResourcesAssociation*, *49*(4), 923-937.

Bunte, K. and Abt, S.R. (2001). Sampling surface and subsurface particle-size distributions in wadable gravel- and cobble-bed streams for analyses in sediment transport, hydraulics, and streambed monitoring. *US Department of Agriculture, Forest Service, Rocky Mountain Research Station*.

Hiller, P.H., Aberle, J. and Lia, L. (2018a). Displacements as failure origin of placed riprap on steep slopes. *Journal of Hydraulic Research*, *56*(2), 141-155.

Hiller, P.H., Lia, L. and Aberle, J. (2018b). Field and model tests of riprap on steep slopes exposed to overtopping. *Journal of Applied Water Engineering and Research*.

Johnson, E.B., Testik, F.Y., Ravichandran, N. and Schooler, J. (2013). Levee scour from overtopping storm waves and scour counter measures. *Ocean engineering*, *57*, 72-82.

Kiplesund, G.H., Ravindra, G.H., Rokstad, M.M. and Sigtryggsdóttir, F.G. (2021). Effects of toe configuration on throughflow properties of rockfill dams. *Journal of Applied Water Engineering and Research*, 1-16.

Larsen, P., Bernhart, H.H., Schenk, E., Blinde, A., Brauns, J. and Degen, F.P. (1986). Uberstrombare Damme, Hochwasserentlastung uber Dammscharten/ Overtoppable dams, spillways over dam notches. *Unpublished Report Prepared for RegierungsprasidiumKarlsruhe, Universita*.

Lia, L., Vartdal, E.A., Skoglund, M. and Campos, H. E. (2013). Rip rap protection of downstream slopes of rock fill dams - a measure to increase safety in an unpredictable future climate. *Paper presented at the European Club Symposium of the International Commission on Large Dams, Venice.*

Najafzadeh, M., Rezaie-Balf, M. and Tafarojnoruz, A. (2018). Prediction of riprap stone size under overtopping flow using data-driven models. *International Journal of River Basin Management*, *16*(4), 505-512.

NVE. (2012). Veileder for fyllingsdammer. *Norwegian Water Resources and Energy Directorate*, 21–25.

Ravindra, G.H., Gronz, O., Dost, B. and Sigtryggsdóttir, F.G. (2020). Description of failure mechanism in placed riprap on steep slope with unsupported toe using smartst one probes. *Engineering Structures*, *221*, 111038.

Ravindra, G.H.R; Sigtryggsdottir, F.G.; Lia, L. (2021). Buckling analogy for 2D deformation of placed ripraps exposed to overtopping. Journal of Hydraulic Research. vol. 59 (1).

Siebel, R. (2007). Experimental investigations on the stability of riprap layers on over toppable earth dams. *Environmental Fluid Mechanics*, *7*(6), 455–467.